Full Paper

Propellants, Explosives, Pyrotechnics

DOI: 10.1002/prep.201500222

The Effect of RDX Crystal Defect Structure on Mechanical Response of a Polymer-Bonded Explosive

Richard H. B. Bouma[a] and Antoine E. D. M. van der Heijden*[b, c]

Abstract: An explosive composition, derived from AFX-757, was systematically varied by using three different qualities of Class I RDX. The effect of internal defect structure of the RDX crystal on the shock sensitivity of a polymer bonded explosive is generally accepted (Doherty and Watt, 2008). Here the response to a mechanical non-shock stimulus is studied using an explosion-driven deformation test as well as the ballistic impact chamber. No correlation between RDX crystal quality and deformation sensitivity is observed. The DDT behavior (Deflagration to Detonation Transition) of the three plastic bonded explosives, although similar in composition, is distinct regarding the rate of diameter increase in the explosion-driven deformation test. Recovered polymer bonded explosive from the explosion-driven deformation test responds equally fast or slower in the ballistic impact chamber. Based on our experimental results the shear rate threshold as a single parameter describing mechanical sensitivity is challenged, and preference is given to the development of an ignition criterion based on intergranular sliding friction under the action of a normal pressure.

Keywords: Crystal defect structure · Polymer bonded explosive · Non-shock deformation

1 Introduction

Non-shock initiation is a major cause of accidents with explosives [1]. Large mechanical deformations are required for the proper functioning of for example some aimable warhead concepts [2], whereas in most munitions applications with energetic materials only minor mechanical deformation is imposed during launch without any negative effect on functioning. In some applications the mechanical deformation is severe and there is a risk of premature functioning. Understanding the non-shock initiation phenomena is the key to prevention of accidents and premature functioning.

A variety of experiments is available to study the mechanical response of explosives at conditions close to or beyond a mechanical initiation threshold. Some experiments mimic particular accident scenarios, like the Susan impact and friability test [3], the Steven impact test [4], the set-back generator [5], and spigot intrusion [6]. In many cases simulations aid the interpretation of the data; specific examples for the split Hopkinson pressure bar, Steven impact, and LANL impact tests can be found in the literature [7–9]. Explosives may be ranked in these experiments according to their threshold values for mechanical initiation (expressed as impact velocity, impact energy, shear rate, etc.) like this is done for thermal, impact, friction, shock, and electrostatic discharge sensitivity. Ranking explosive compositions by their hazard properties has enabled the introduction of new explosive compositions, like in the replacement of tetryl, which was the separation between booster and high explosive [10], and the direct comparison of munition vulnerabilities, like in a specific low velocity impact scenario [11]. Note that the ingredients of an explosive composition and their amounts are indicative for sensitivity only to a limited extent. These composition details do not reveal product properties like defect content, particle shape, purity, etc. and cannot explain the underlying mechanisms that lead to initiation and the severity of the subsequent reaction [12]. These mechanisms need to be understood in order to explain similarities or differences between various experiments or quantify the possibility of ignition in an accident scenario.

[a] *R. H. B. Bouma*
Department Process Instrumentation and Design
TNO, Organisation for Applied Scientific Research
P.O. Box 6012
2600 JA, Delft, The Netherlands

[b] *A. E. D. M. van der Heijden*
Department Energetic Materials
TNO, Organisation for Applied Scientific Research
P.O. Box 45
2280 AA Rijswijk, The Netherlands
**e-mail: antoine.vanderheijden@tno.nl*
a.e.d.m.vanderheijden@tudelft.nl

[c] *A. E. D. M. van der Heijden*
Section Intensified Reaction and Separation Systems
Delft University of Technology
Leeghwaterstraat 39
2526 CB Delft, The Netherlands

In a particular shear impact experiment on the polymer bonded explosive PBX9501 Skidmore et al. [13] observed both inter- and intra-crystalline sliding motion. The question was not resolved, which mechanism was responsible for stimulation of thermal ignition. Coffey and co-workers stress the importance of intra-crystalline sliding friction. According to Coffey [14] the hot spot generation in crystalline explosives under shock and impact conditions follows the same physical process and involves the localization of moving dislocations into shear bands. Shear rate thresholds for initiation of energetic crystals and explosive compositions were determined from ballistic impact chamber experiments [15], using sample dimensions, drop weight velocity, and time-to-reaction. For inter-granular sliding friction, Browning [16] developed a model that links mechanical properties and particles sizes to the thermal ignition. The ignition criterion is based on the Hertz contact stress between particles, the mechanical work in the particles contact surface due to sliding motion, and thermo-chemical decomposition due to the locally deposited heat [8, 9, 16].

The mechanical deformation of a PBX and its sensitivity to ignition is studied here, applying two different experimental set-ups, namely the ballistic impact chamber and the explosion-driven deformation test. An explosive composition, derived from AFX-757, was systematically varied by using Class I RDX from three different sources and with known differences in crystal quality. RDX from the same sources had been used previously in an international Reduced Sensitivity RDX Round Robin program to study the relation between properties of the RDX crystals and the shock sensitivity of the composition PBXN-109 with 64% of the various RDX qualities [17]. The RDX crystal quality has a tremendous effect on the shock sensitivity of PBXN-109. Herein the effect of RDX crystal quality on non-shock initiation of a PBX is the topic of research, more specifically, the assessment whether the shock sensitivity of a PBX is also indicative of its sensitivity to mechanical deformation.

2 Material and Methods

2.1 Polymer-Bonded Explosive

Three PBXs were prepared by mixing and casting with a HKV5, 1 gallon mixer. The ingredients were 25% by weight of Class I RDX, 33% aluminum AS081, 30% ammonium perchlorate of 200 μm mean particle diameter, embedded in a hydroxyl terminated polybutadiene (HTPB) binder system. The particulate content is thus 88% and the binder content 12%. The composition of the PBX resembles but is not exactly equal to AFX-757 [18]. An important difference is the RDX. The specification of AFX-757 prescribes the use of 5% Type II Class I RDX and 20% Type II 4 μm RDX. In this paper the effect of RDX quality on mechanical response is the topic of research and 25% of Class 1 RDX was used. The RDX originated from the international Reduced Sensitivity RDX Round Robin program [17,19], from which three different qualities were selected. The defects in the RDX grades were investigated with optical microscopy, scanning electron microscopy and confocal scanning laser microscopy [20].

Table 1. Identification of PBX, source of RDX Class I crystal in the PBX, and the measured PBX density. The RDX sample codes from the international Round Robin program are put in brackets for comparison with literature [17, 20].

PBX	RDX source	Density PBX [kg m^{-3}]
RU185	ADI (K7)	$(1.85–1.87)\times10^3$
RU186	Dyno Type II (K6)	$(1.83–1.84)\times10^3$
RU187	BAe Royal Ordnance (K1)	$(1.84–1.85)\times10^3$

Table 2. Specifications of RDX Class I crystals used in the PBX formulations (see Table 1) [20].

	RDX K1	RDX K6	RDX K7
Density RDX [g cm^{-3}]	1.795	1.804	1.794
Shock initiation pressure [GPa]	5.06	3.86	5.21
Quality	intermediate	bad	good
Macro-inclusions	yes	yes, many	hardly
Micro-inclusions	yes, few	yes, many[a)]	yes
Intra-granular voids	no	no	yes
Cracks	no	no	yes
Growth bands	no	yes	yes
Growth sectors	no	yes	Yes

a) Including micro-inclusions aligned as a "pearl necklace", see Figure 1b [20].

Table 1 provides an identification number, source of the RDX, and measured density of the PBXs. The composition-specific shock sensitivity of PBXN-109 with RDX from ADI, Dyno (Type II), and BAe Royal Ordnance was 5.21, 3.86, and 5.06 GPa, respectively [19]. Table 2 summarizes specifications of RDX crystals used and the type of defects that were typically found in these crystals, as observed with optical, scanning electron and confocal scanning laser microscopy. Examples of these three microscopic techniques applied to the RDX variants of this study are shown in Figure 1. For details on the preparation of these samples, see Ref. [20].

2.2 Explosion-Driven Deformation

Explosion-driven deformation tests were performed in two configurations. Figure 2 shows the standard geometry. From left to right there is a 5 cm steel cylinder filled with sand, a 10 cm steel cylinder filled with the PBX, and a 5 cm steel tube filled with sand. The sand-filled cylinders provide an impedance match and thus a homogeneous deformation of the central PBX-filled cylinder. The cylinders were made out of St 52 and have an internal and external diameter of 60 and 70 mm respectively. A layer of plastic explosive around one-third of the circumference of the cylinder was used to drive the deformation of the steel-encased

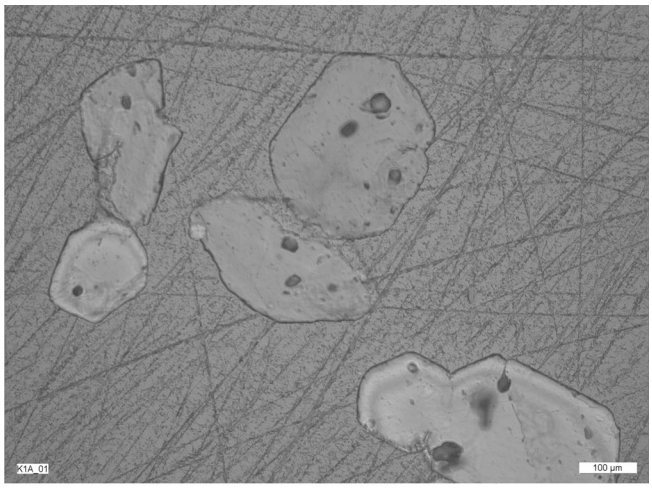

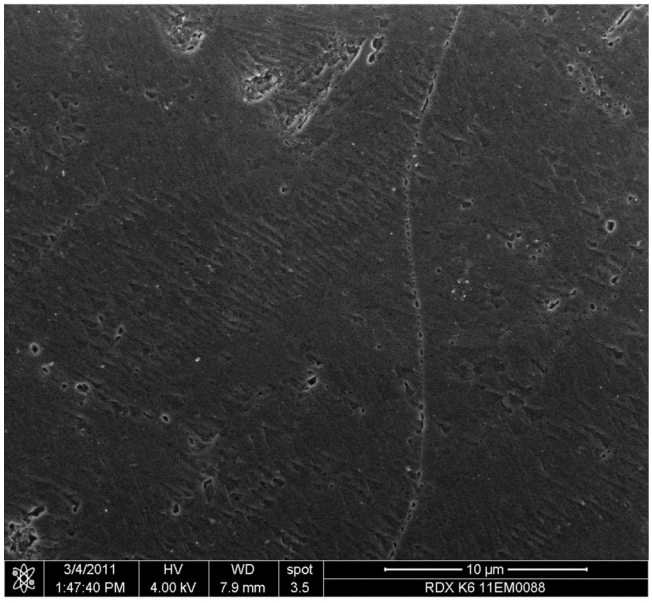

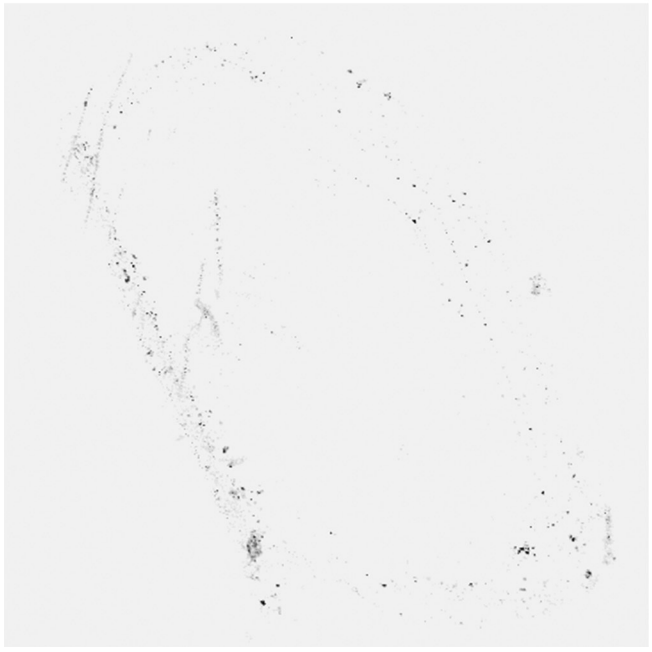

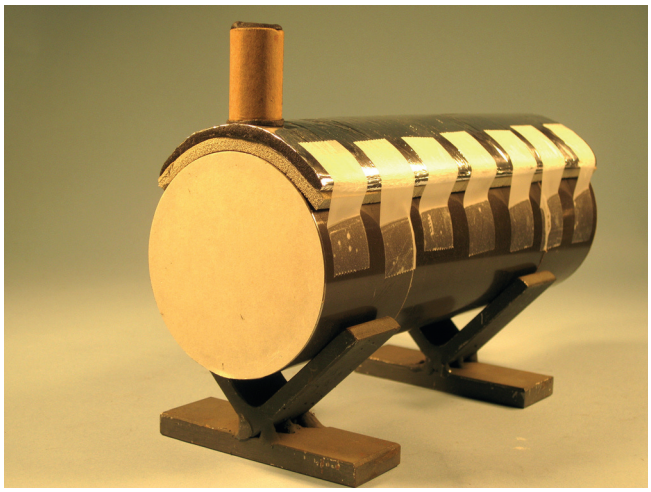

Figure 2. Explosion-driven deformation test with plastic explosive layer deforming a steel-encased PBX.

PBX. The thickness of the Semtex 10 plastic explosive layer was varied. A 4 mm thick rubber foam layer was put in between the Semtex 10 layer and the steel cylinder, and had to prevent a direct shock initiation of the PBX. A detonator was inserted in a small amount of plastic explosive, visible at the left in Figure 2, to initiate a detonation and start the deformation process. The detonation of the plastic explosive progressively deformed the three steel cylinders. The punch marks in the steel cylinders near the sand/PBX interface and the PBX/sand interface show the progress of deformation from recovered fragments. The PBX was deformed as well and may have reacted to a certain extent. In the elongated geometry there were two instead of one 10 cm long PBX-filled cylinders. The experiment was carried out with the configurations placed on top of a triangular ridge of sand that can give way in order to minimize the resistance to deformation; the deformation is predominantly imposed by the work exerted by the detonating plastic explosive.

The explosion-driven deformation test has been applied before to PBXN-109, consisting of 64 wt% RDX and 20% aluminum, and to a PBX with 70% of RDX or I-RDX® [21,22]. With PBXN-109 a transition from deformation to deformation plus partial reaction of the explosive was observed with an increase of the plastic explosive layer thickness from 3 to 5 mm. With the 70% RDX-containing PBX larger deformation could be achieved, albeit without any reaction. Results demonstrated that a PBX should have a sufficiently high particulate content, for the applied steel case thickness, in order for a reaction to develop.

Figure 1. (a) Optical micrograph in incident light mode of RDX K1 crystals. (b) Scanning electron micrograph of a single, cleaved RDX K6 crystal. (c) Inverted confocal scanning laser micrograph (375× 375 µm) of a single RDX K7 crystal. For typical type of defects in these crystals, see Table 2.

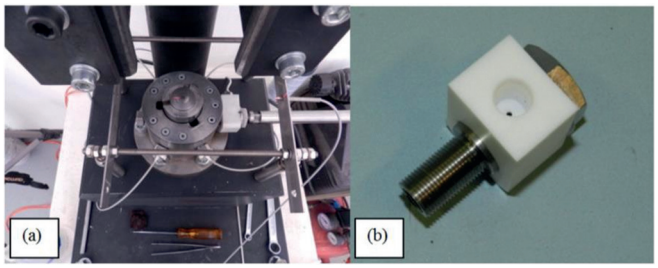

Figure 3. (a) Top view of ballistic impact chamber. A laser light strikes the top surface of the striker. Four optic fibers with photodiodes are placed in the chamber to monitor the start of a reaction. (b) The pressure transducer to monitor the blast overpressure is mounted in a Teflon block that can freely rotate on a metal threaded insert that connects the chamber and the pressure relief barrel.

2.3 Ballistic Impact Chamber

The ballistic impact chamber is an instrumented impact machine. Instead of measuring the 50% probability of initiation of an explosive sample by variation of a drop weight, it measures the growth and extent of a reaction under a standard impact condition [23]. When the drop weight (9.983 kg) is released from a height of 1.5 m, it will impact a striker (mass 229 g) and start the deformation of the explosive sample positioned directly underneath the striker on top of an anvil. The time-to-reaction after the start of the deformation, and the pressure evolution in the chamber confined by anvil and striker, were measured. The occurrence of a reaction was monitored with four optic fibers with photodiodes (see Figure 3a). The time-to-reaction corresponds to the first photodiode signaling a reaction. The reaction starts near the outer radius of the compressed sample, as concluded by observations made in similar experiments [15]. The blast overpressure was measured now at the position, where the reaction products leave the chamber through a barrel which acts as automatic pressure relief (see Figure 3b). This is a modification to earlier experiments where a reflected pressure was measured opposite to the pressure relief barrel [24]. In the previous configuration one could not tell whether the measured pressure was representative for the whole chamber; the actual pressure might be higher. In the current configuration one is certain that the pressure is representative for the pressure in the chamber as the gases have to pass by the pressure transducer when leaving through the barrel. The new configuration will avoid the occurrence of pressure spikes associated with a direct impact of blast wave and particles onto the diaphragm of the pressure transducer, while better monitoring the dynamics of the pressure evolution in the chamber. Samples were prepared by punching out a cylinder from a slice of PBX, and polishing both surfaces with subsequently finer grit sand papers to obtain plane-parallel surfaces of the desired thickness.

The use of a 180 grit sand or garnet paper is mentioned in the literature [25] to standardize and enhance the friction of the explosive sample on the anvil. The influence of the sandpaper was verified herein using a relatively thick 180 grit paper with textile backing, a thin 180 grit polishing paper (Buehler) and without sand paper. Tests were performed in triplicate with RU185 samples having a dimension of 3.5 mm Ø×2.5 mm or 5.0 mm Ø×2.4 mm. The 180 grit polishing paper gives the shortest average time-to-reaction of 0.33 ms for both diameters. A slightly longer time-to-reaction is observed without the use of sandpaper between RU186 and anvil. The 180 grit paper with textile backing gave the longest time-to-reaction of about 0.43 to 0.44 ms. Apparently there is a difference in the way friction by the two types of polishing paper is imposed onto the explosive sample. It was decided to continue the experiments with the 180 grit polishing paper as it enhances friction with respect to the bare anvil.

2.4 Deformation by Dropweight Impact

Apart from the samples resulting from the explosion-driven deformation experiments, samples taken from the original PBXs were subjected to a drop weight impact test. The aim of this test is to impose a mechanical deformation onto the PBX like in the explosion-driven deformation test, only at a lower compression rate. This drop weight impact test was performed with an 18 mm Ø×10 mm sample attached to the lower surface of a 9.895 kg drop weight, which was released from 2.24 m onto a steel anvil. A 5 mm thick retaining ring with 40 mm internal diameter, limited the final compression, but allowed for free radial expansion. By comparison to the dimensions and impact condition in the UN friability test [3] it was anticipated that no reaction would occur.

3 Results

The mechanical response of PBX samples was tested with the ballistic impact chamber and the explosion-driven deformation test. The mechanical response in the ballistic impact chamber was also tested with PBX samples that were subjected to severe mechanical loading near the mechanical initiation threshold.

3.1 Explosion-Driven Deformation

In the explosion-driven deformation test the degree of deformation of the metal cylinder increases with thickness of the plastic explosive layer. The deformation along the PBX containing steel cylinder was almost constant for a 3 or 4 mm Semtex layer. With a layer of 5 mm or more, the compression of the metal cylinder was counteracted by an internal pressure due to the ignition of the PBX and growth of reaction, resulting in a non-constant deformation along the steel cylinder. Figure 4 presents the amount of recovered explosive as a function of the applied explosive

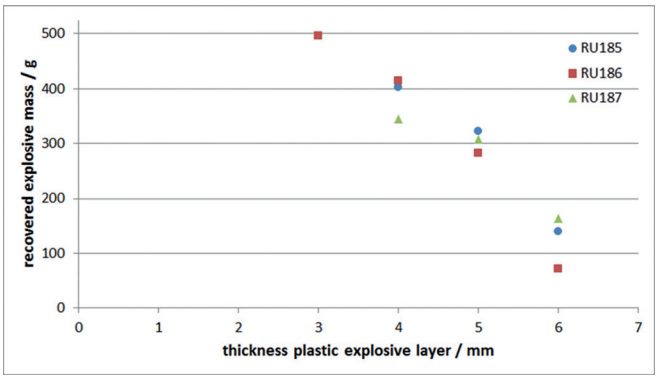

Figure 4. Amount of recovered explosive vs. the thickness of the plastic explosive layer in the explosion-driven deformation test.

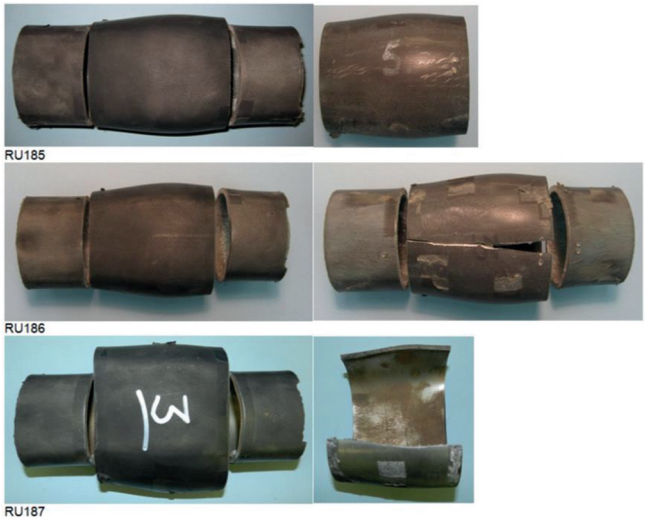

Figure 5. Steel cylinders after explosion-driven deformation with 5 mm Semtex layer, with deformation proceeding from left to right. From top to bottom are the experiments with RU185, RU186, and RU187. At the left are the photographs of the cylinder surface underneath the deforming layer, at the right are the photographs taken from the opposite side.

Figure 6. Steel cylinders after explosion-driven deformation with 5 mm Semtex layer in elongated configuration. From top to bottom are the experiments with RU185, RU186, and RU187, respectively.

layer thickness. The initial PBX mass in a 10 cm cylinder was in the range of 517 to 528 g. The experiments covered the range of almost no reaction to almost full reaction of the PBX.

Figure 5 shows the recovered metal in the explosion-driven deformation by a 5 mm Semtex layer in the standard geometry. The detonation has propagated from left to right in the photographs. Typical in all experiments was the imprint of the structure of the rubbery foam along all three cylinders and the spallation observed in the last sand-filled cylinder, which was due to the abrupt end of the detonation near the steel free surface. A start of a reaction is observed as the metal cylinder starts expanding. Differences in the violence of the reaction are inferred from the fracturing behavior. The cylinder with RU185 shows a bulge, the cylinder with RU186 has a fracture running backwards from the right, and the cylinder with RU187 is fully split along its length. A maximum expansion is observed at 2/3 of the 10 cm long cylinder. It was expected that from the moment the compression wave passed the second PBX-sand interface pressure in the PBX was relieved, thereby suppressing a further conversion of the energetic material. This hypothesis was verified by performing experiments in an elongated geometry with two PBX-filled cylinders.

Figure 6 shows the recovered metal in the explosion-driven deformation by a 5 mm Semtex layer in the elongated geometry. With the RU185 sample a continued increase in reaction strength is noticed. The first cylinder is now split in two parts, and the second cylinder in four parts, and several other cracks in the axial direction are visible. An advantage of the elongated geometry with two cylinders instead of one longer cylinder is the fact that fracture cannot grow across the interface and the global shape of the first cylinder is "maintained", and thus capable of showing the start of reaction. The "diameter" of the first cylinder does not pass through a maximum but is now strongly increasing. The RU186 sample shows a comparable fracturing behavior. Surprisingly, the RU187 sample which was the most violent in the standard geometry, demonstrates an increase of diameter in the first cylinder as well as a decrease

Figure 7. Left: RU187 cylindrical sample and retaining ring attached with double-sided tape to drop weight (top). Right: permanent deformation of the samples after drop weight impact.

of diameter near the end of the second cylinder, and is not able to sustain the reaction.

3.2 Ballistic Impact Chamber

The mechanical response in the ballistic impact chamber was tested using samples with different dimensions. The sample mass was about 43 mg for the 3.5 mm Ø×2.5 mm samples and about 80 mg for the 5.0 mm Ø×2.4 mm samples. The tested samples were taken from the as-cast PBX, from recovered explosive in the explosion-driven deformation test with 4 and 5 mm of Semtex, and from the explosive recovered after a drop weight impact test. The latter drop weight impact test is shown in Figure 7. Permanent deformation of the samples remains after impact and causes a few vertical cracks on the outer radius (see Figure 7).

The time-to-reaction in the ballistic chamber of pristine and mechanically loaded samples is given in Table 3. Recovered PBX from the explosion-driven deformation test responded equally fast or slower in the ballistic impact chamber. In particular for RU185 the time-to-reaction increased upon mechanical loading. RU185 and RU186 recovered from the drop weight impact, show an even further increase in time-to-reaction in the ballistic impact chamber. One can calculate the time to reduce the sample to zero thickness by dividing sample thickness and striker velocity assuming that mechanical properties of the PBX are of no importance in compression. The compression is driven by the velocity of the striker, which in turn depends on the impact velocity of the drop weight.

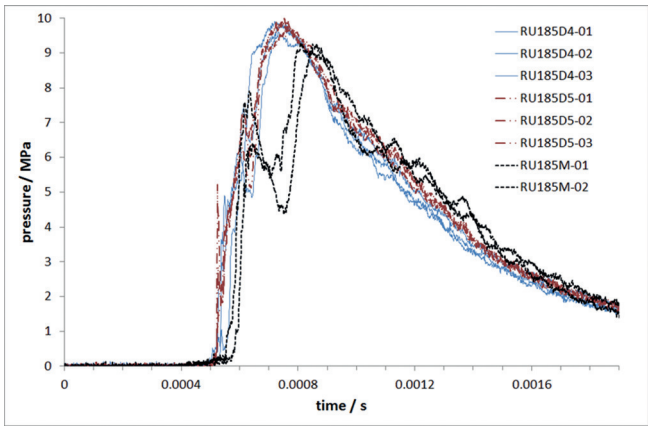

Figure 8. Mechanical response of 3.5 mm Ø×2.5 mm RU185 samples in ballistic impact chamber. Samples were taken from the explosion-driven deformation tests with a 4 mm (RU185D4-xx) or 5 mm (RU185D5-xx) plastic explosive layer, and from the drop weight impact test (RU185M-xx). Time scales are relative to the start of deformation measured for each individual experiment.

$$v_{\text{striker}} = 2v_{\text{dropweight at impact}} \frac{m_{\text{dropweight}}}{m_{\text{dropweight}} + m_{\text{striker}}}$$

The velocity of the drop weight at impact is 5.35 m s^{-1}, when the 9.983 kg drop weight is released from 1.5 m. The mass of the striker is 229 g. The times to compress the sample to zero thickness are thus 0.23 and 0.24 ms for the 2.4 and 2.5 mm sample thicknesses, respectively. These times are smaller than the measured times to reaction in Table 3.

Figure 8 and Figure 9 show the reproducibility of pressure measurements in the new configuration. This is also confirmed by calculating the time integral of the pressure. No significant differences are noticed in the pressure-time response shown in Figure 8 when using a 4 or a 5 mm thick plastic explosive layer in the explosion-driven deformation. In Figure 8 the RU185 samples recovered from the drop weight impact show a delay in the moment that pressure starts to increase in comparison to samples from explosion-driven deformation, a result which is in line with the respective optically determined times to reaction in Table 3.

Table 3. Sensitivity of PBX samples in ballistic impact chamber expressed as time-to-reaction, for indicated experimental conditions: as-cast, deformation with 4 mm and 5 mm Semtex, after deformation by drop-weight.

Sample	Ø×h [mm]	Time-to-reaction [ms]			
		As-cast	4 mm Semtex	5 mm Semtex	Drop weight
RU185	3.5×2.5	0.32–0.35	0.41–0.43	0.43–0.45	0.44–0.46
RU186	3.5×2.5	0.35–0.43	0.40–0.42	0.38–0.45	0.47–0.48
RU187	3.5×2.5	0.39–0.41	0.37–0.39	0.39–0.42	0.42–0.43
RU185	5.0×2.4	0.31–0.35	0.40–0.44	0.40–0.43	0.44–0.48
RU186	5.0×2.4	0.27–0.40	0.38–0.40	0.43–0.45	0.45
RU187	5.0×2.4	0.41–0.43	0.37–0.39	0.40–0.42	0.41–0.42

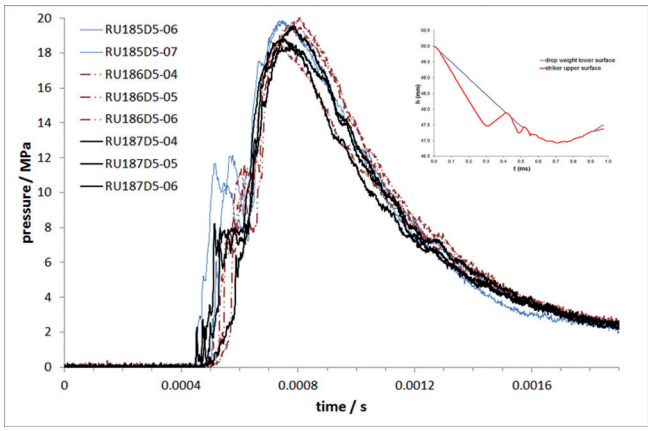

Figure 9. Mechanical response of 5.0 mm Ø×2.4 mm PBX samples in ballistic impact chamber in triplicate experiments. Samples were taken from the explosion-driven deformation tests with a 5 mm plastic explosive layer (RU185/186/187D5-xx). The inserted Figure provides the positions of the striker upper surface and drop weight lower surface from numerical simulation of impact on an explosive of similar dimensions.

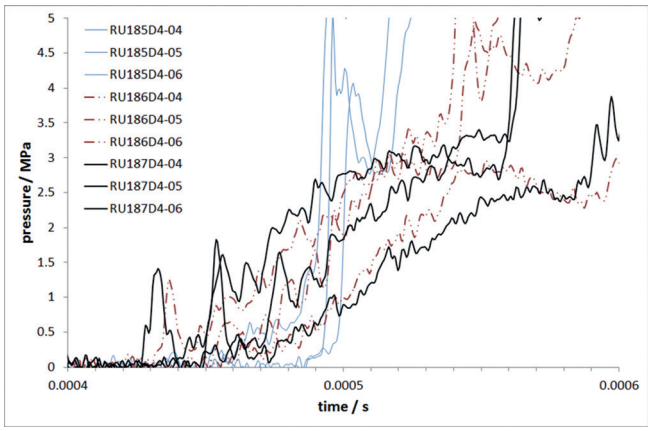

Figure 10. Initial mechanical response of 5.0 mm Ø×2.4 mm PBX samples in ballistic impact chamber in triplicate experiments. Samples were taken from the explosion-driven deformation tests with a 4 mm plastic explosive layer (RU185/186/187D4-xx).

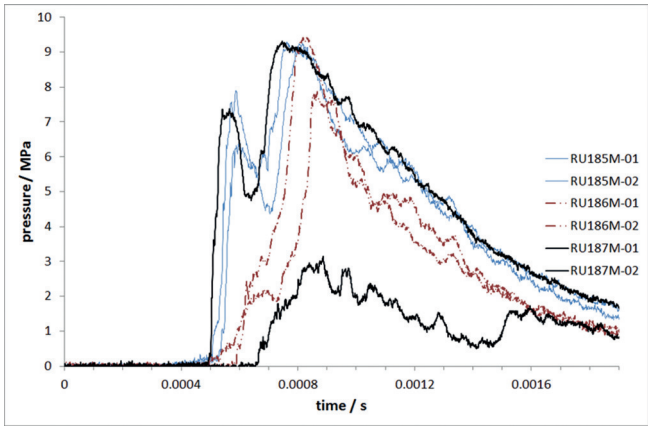

Figure 11. Mechanical response of 3.5 mm Ø×2.5 mm samples in ballistic impact chamber. Samples were taken from the drop weight impact test (RU185/186/187M-xx). Time scales are relative to the start of deformation measured for each individual experiment.

Figure 9 shows the pressure evolution for the three different PBXs in case of deformation with 5 mm of plastic explosive. The order, in which pressure starts to build-up, is RU185, RU187, and RU186, respectively. The time lag between the moment of first reaction measured by the photodiodes and the moment pressure builds up, is of the right order given the distance between the explosive and the pressure sensor, and the sound velocity in air. The insert of Figure 9 is a simulation of the compression of a 5.0 mm Ø×2.4 mm non-reactive high explosive, with initially a 0.1 mm air gap above and below the explosive for numerical purposes. The inserted figure demonstrates how the striker rebounds between anvil and drop weight until at 0.7 ms both striker and drop weight achieve an upward velocity. The volume fluctuations in the impact chamber between 0.3 and 0.7 ms will directly impose a pressure fluctuation in the chamber on top of the pressure generated by the decomposing explosive. It is striking to see (1) the experimental pressure build-up is noticed only after 0.45 ms, when the numerical simulation shows a first rebound of the striker against the falling drop weight, (2) a plateau in the pressure near 0.5 ms, when the simulation shows the second rebound of the striker against the anvil, and (3) an experimental maximum pressure near 0.85 ms coinciding with the inversion of the drop weight velocity near 0.7 ms in the simulation. Because of the complex striker movement, sample compression and dynamic volume of the chamber, one has to be careful to infer an order of sensitivity from the start of the pressure build-up.

Figure 10 shows the initial pressure rise for the three different PBXs in case of deformation with 4 mm of plastic explosive. By zooming in, it is observed that the RU185 samples are characterized by a delayed pressure build-up with respect to RU186 and RU187. The pressurization rate for RU185, however, is larger. For RU186 and RU187 the initial pressure rise to 2.5 MPa occurs in ca. 0.1 ms, a time-scale comparable or larger than the rebound of the striker. The lower pressurization rate is therefore assumed to be related to the lower deflagration rate in the RU186 and RU187 samples.

The mechanical response of 3.5 mm Ø×2.5 mm samples from PBX recovered from the drop weight impact is shown in Figure 11. RU185 shows a consistent and fast pressure build-up. RU186 shows a delayed response. The response of RU187 is again inconsistent. It may react as fast as RU185 or even slower than RU186.

4 Discussion and Conclusions

The response to a mechanical non-shock stimulus was studied with an explosive composition, derived from AFX-757, using an explosion-driven deformation test as well as the ballistic impact chamber. The crystal quality of the RDX particles embedded in the polymer bonded explosive was varied, and the expected order from high to low shock sensitivity is RU186, RU187, and RU185, respectively, with only a marginal difference between the latter two. This expectation is based on measured shock sensitivities of PBXN-109 with seven different qualities of RDX [19, 20], from which three qualities were included in this study. The question is whether the shock sensitivity of a PBX is also indicative of its sensitivity to mechanical deformation.

The DDT behavior (Deflagration to Detonation Transition) of the three plastic bonded explosives, although similar in composition, is distinct regarding the rate of diameter increase in the explosion-driven deformation test. RU185 and RU186 are comparable in mechanical response with RU186 being slightly more violent in the explosion-driven deformation test. Even though changes are noticed in the expansion of the metal cylinder, no clear differences between PBXs are noted from the amount of recovered explosive after an explosion-driven deformation test, using different thicknesses of the Semtex layer of 3, 4, 5, and 6 mm. In the explosion-driven deformation it is RU187 that demonstrates the most violent response in the standard geometry, albeit the reaction does not sustain itself in the elongated geometry. RU187 therefore requires a heavier confinement than RU185 and RU186 to sustain and accelerate a reaction. In the ballistic impact chamber the insensitivity to mechanical deformation, as expressed in time-to-reaction, is the highest for RU187. RU185 reacts much faster than RU187. For RU186 the variation in time-to-reaction is quite large and one cannot distinguish RU186 from either RU185 or RU187. The moment pressure starts to increase as well as the pressurization rate in the ballistic impact chamber [25], are not used in the interpretation of the experimental data, because of the volume fluctuation due to repetitive striker rebounds as found in numerical simulations. Altogether, it is concluded that there is no correlation between shock sensitivity and sensitivity towards mechanical deformation based on the experimental data presented herein.

The expansion of the metal cylinder due to mechanical initiation and propagation of a deflagration in the PBX has an analogue in the so-called DDT test tubes. In DDT tests the deflagration is imposed by an ignition wire or ignition capsule, see, for example Test Series 5 in [3]. In Ref. [26] the tube expansion in DDT beyond the elastic regime is studied analytically and numerically through a model experiment. Iso-damage curves are constructed providing information on pressure and impulse per unit area necessary to achieve a certain amount of plastic strain. The same concept can be applied to the expansion in the explosion-driven deformation test, where ideally the pressure and impulse per unit area should be related to the local fraction of reacted explosive as depicted in Figure 4. The impulse per unit area equals the time integral of internal pressure in the cylinder and can be approximated by the product of peak pressure and a typical time scale. The time scale to transfer impulse from the reaction products to the metal cylinder is expected to be dominated by the length of the PBX-filled cylinder divided by the detonation velocity of Semtex 10 (i.e. 100 mm/7.3 mm/μs = 13.6 μs). Note that this time scale is less than one tenth of the time scale for initiation in the ballistic impact chamber.

Both in shock-to-detonation transition (SDT) and DDT in explosives one should distinguish between the initiation of a reaction and the growth and acceleration of the reaction [27]. Crystal related features that affect shock sensitivity (like presence of micron size defects or number density of submicron size defects) may not be the same as the features that affect growth and acceleration of the reaction (like specific surface, internal crystal defects). The shear rate threshold $\partial\gamma/\partial t$ for ignition of energetic materials is evaluated by [15], applying the following equation to the experimental results with the ballistic impact chamber:

$$\frac{\partial \gamma}{\partial t} \approx \frac{r(t=0)}{h\left(t=t_{ign}\right)^2}\sqrt{\frac{h(t=0)}{h\left(t=t_{ign}\right)}}\cdot\frac{\partial h}{\partial t}\left(t=t_{ign}\right)$$

with r and h the radius and height of the sample, t_{ign} the moment of ignition is observed relative to the start of deformation. This model is derived from the hypothesis that intra-granular shear deformation being responsible for ignition. For RU185, RU186, and RU187 the times to reaction always exceed the sample thickness divided by striker velocity, and the above equation cannot be applied. Based on our experimental results, the shear rate threshold as parameter describing mechanical sensitivity is therefore challenged. Instead of intra-granular, inter-granular shear deformation is another mechanism that may lead to ignition. In its earliest form [16], the ignition criterion for an HMX based explosive is derived by combining (1) the analytical equations for the Hertz contact stress between particles, (2) the mechanical work in the particles contact surface due to sliding motion, and (3) with the numerical simulation of thermo-chemical diffusion and decomposition processes due to the locally deposited heat.

In a particular example the threshold for mechanical initiation of an HMX-based explosive was found to be [16]:

$$\textit{Mechanical ignition threshold} = p^{0.66}\cdot\frac{\partial \gamma}{\partial t}^{1.27} t_{ign}{}^{0.27}$$

The pressure and shear rate during mechanical loading will be time-dependent [28]. For this reason further devel-

opments include the incorporation of time-variable pressure p and shear rate $\partial\gamma/\partial t$ into a more generic model [8].

Mechanical ignition threshold

$$= \int_0^{t_{ign}} \left(\frac{t_{ign} - \tau}{t^*}\right)^{-n} \left(\frac{p(\tau)}{p^*}\right)^{\frac{2n}{3}} \frac{\partial\gamma}{\partial t}(\tau)\, d\tau$$

with p^* a characteristic pressure, t^* a characteristic time, and the exponent n related to the decomposition kinetics of the specific explosive. The same authors validated the improved model using low velocity impact experiments on HMX-based compositions in different geometries of the Steven Impact test. No ignition criterion is found yet in literature for RDX based compositions. Based on the experimental results presented in this paper, preference is given to the development of such an ignition criterion based on inter-granular sliding friction under normal pressure [8, 9, 16, 29] rather than intra-granular shear deformation, preferably incorporating the friction coefficients of RDX crystals [30].

Acknowledgments

The authors acknowledge support from the U.S. Defense Threat Reduction Agency under project award HDTRA1-10-1-0078. Rudie Krämer, John Makkus and Arien Boluijt are acknowledged for assistance with the preparation of PBXs, explosion-driven deformation and ballistic impact chamber experiments.

References

[1] B. W. Asay, *Introduction in Non-Shock Initiation of Explosives* (Ed.: B. W. Asay), Springer, New York, ISBN 978-3-540-87952-7, **2010**.
[2] R. M. Lloyd, Conventional Warhead Systems Physics and Engineering Design, *34th AIAA/ASME/SAE/ASEE Joint Propulsion Conference and Exhibit*, Cleveland, OH, USA, July 13–15, **1998**, AIAA Paper 1998-179.
[3] ST/SG/AC.10/11/Rev.5, *Recommendations on the Transport of Dangerous Goods. Manual of Tests and Criteria*, United Nations, New York, **2009**.
[4] S. K. Chidester, C. M. Tarver, R. Garza, Low Amplitude Impact Testing and Analysis of Pristine and Aged Solid High Explosives, *11th Symposium (International) on Detonation*, Snowmass Village, CO, USA, August 31–September 4, **1998**.
[5] H. W. Sandusky, P. G. Chamber, V. J. Carlson, Setback Simulation of Fielded and Candidate Explosive Fill for 5"/54 Guns, *JANNAF Propulsion Systems Hazards Subcommittee Meeting*, Tucson, AZ, USA, 7–11 December, **1998**, CPIA Publ. 681, Vol. II, 137–145.
[6] I. G. Wallace, Spigot Intrusion, *26th Department of Defense Explosives Safety Seminar*, Miami, FL, USA, August 16–18, **1994**.
[7] P. Bailly, F. Delvare, J. Vial, J. L. Hanus, M. Biessy, D. Picart, Dynamic Behavior of an Aggregate Material at Simultaneous High Pressure and Strain Rate: SPHB Triaxial Tests, *Int. J. Impact. Eng.* **2011**, *38*, 73–84.
[8] C. Gruau, D. Picart, R. Belmas, E. Bouton, F. Delmaire-Sizes, J. Sabatier, H. Trumel, Ignition of a Confined High Explosive under Low Velocity Impact, *Int. J. Impact. Eng.* **2009**, *36*, 537 – 550.
[9] R. J. Scammon, R. V. Browning, J. Middleditch, J. K. Dienes, K. S. Haberman, J. G. Bennett, Low Amplitude Insult Project: Structural Analysis and Prediction of Low Order Reaction, *11th Symposium (International) on Detonation*, Snowmass Village, CO, USA, August 31–September 4, **1998**.
[10] J. Pisano, *Assessment of Hazard Properties of Tetryl Replacement Formulations*, DSTO Materials Research Laboratory Technical Report MRL-TR-90-21, Canberra, Australia, **1990**.
[11] K. S. Vandersall, L. L. Switzer, F. Garcia, Thresholds Studies on TNT, Composition B, C-4 and ANFO Explosives Using the Steven Impact Test, *13th Symposium (International) on Detonation*, Norfolk, VA, USA, July 23–28, **2006**.
[12] A. E. D. M. van der Heijden, R. H. B. Bouma, *Energetic Materials: Crystallization and Characterization, in: Handbook of Material Science Research* (Eds.: C. Rene, E. Turcotte), Nova Science Publishers, Hauppauge, **2010**.
[13] C. B. Skidmore, D. S. Phillips, B. W. Asay, D. J. Idar, P. M. Howe, D. S. Bolme, *Microstructural Effects in PBX9501 Damaged by Shear Impact*, Los Alamos Report LA-UR-99-32338, Los Alamos, NM, USA, **1999**.
[14] C. S. Coffey, The Initiation of Explosive Crystals by Shock or Impact, *J. Physique* **1987**, C4 253 – 263.
[15] J. Namkung, C. S. Coffey, *Plastic Deformation Rate and Initiation of Crystalline Explosives, Proceedings of Shock Compression of Condensed Matter*, CP620, American Institute of Physics, **2001**, 1003 – 1006.
[16] R. V. Browning, Microstructural Model of Mechanical Initiation of Energetic Materials. *Proceedings of APS Conference on Shock Compression of Condensed Matter*, Seattle, WA, USA, August 13–18, **1995**.
[17] D. Watt, R. Doherty, L. Nock, *RS-RDX Round Robin (R4) Preliminary Results Analysis*, NATO-MSIAC Report L-127, **2006**.
[18] MIL-DTL-32074 (USAF), *Explosive, Plastic-Bonded, Cast AFX-757*, Notice 1, 30 April **2002**.
[19] R. M. Doherty, D. S. Watt, Relationship Between RDX Properties and Sensitivity, *Propellants Explos. Pyrotech.* **2008**, *33*, 4.
[20] R. H. B. Bouma, W. Duvalois, A. E. D. M. van der Heijden, Microscopic Characterization of Defect Structure in RDX Crystals, *J. Microscopy* **2013**, *252*, 263 – 274.
[21] R. H. B. Bouma, A. E. D. M. van der Heijden, T. D. Sewell, D. L. Thompson, *Simulations of Deformation Processes in Energetic Materials, in Numerical Simulations of Physical and Engineering Process* (Ed.: J. Awrejcewicz), Intech, Rijeka, **2001**, ISBN: 978-953-307-620-1.
[22] D. Meuken, M. Martinez Pacheco, H. J. Verbeek, R. H. B. Bouma, L. Katgerman, Shear Initiated Reactions in Energetic and Reactive Materials, *Mater. Res. Soc., Symp. Proc.*, Boston, MA, USA, November 27–December 1, **2006**, 896, 0896-H06-06.
[23] C. S. Coffey, V. F. DeVost, Impact Testing of Explosives and Propellants, *Propellants Explos. Pyrotech.* **1995**, *20*, 105 – 115.
[24] R. H. B. Bouma, A. G. Boluijt, H. J. Verbeek, A. E. D. M. van der Heijden, *On the Impact Testing of Cyclotrimethylene Trinitramine Crystals*, *J. Appl. Phys.* **2008**, *103*, 093517.
[25] C. S. Coffey, V. F. DeVost, *Impact Testing of Explosives and Propellants*, Report NSWCDD/TR-92/280, Naval Surface Warfare Center, Dahlgren, VA, USA, **1992**.
[26] J. E. Shepherd, F. Pintgen, *Elastic and Plastic Structural Response of Tubes to Deflagration-to-detonation Transition*, Report FM2006-005, California Institute of Technology, Pasadena, CA, USA, **2007**.

[27] E. L. Lee, C. M. Tarver, Phenomenological Model of Shock Initiation in Heterogeneous Explosives, *Phys. Fluids* **1980**, *23*, 362 – 2372.
[28] R. V. Browning, R. J. Scammon, Microstructural Model of Ignition for Time Varying Loading Conditions. *Proceedings of Shock Compression of Condensed* Matter (Eds.: M. D. Furnish, N. N. Thadhani, Y. Horie), CP620, American Institute of Physics, **2001**.
[29] F. Delmaire-Size, R. Belmas, C. Gruau, D. Picart, H. Trumel, Pyrotechnic Safety: Low-Velocity Impact Consequences, *Revue Scientifique et Technique de la Direction des Applications Militaires du CEA*, 38, **2010**.
[30] Y. Q. Wu, M. Munawar Chaudhri, Coefficients of Sliding Friction of Single Crystals of High Explosives under Different Rubbing Conditions, *J. Phys. D Appl. Phys.* **2013**, *46*, 035303.

Received: August 21, 2015
Revised: October 2, 2015
Published online: November 9, 2015

